Kevin Davis; John G Hayes "Fuel cell vehicle energy management strategy based on the cost of ownership"

Research article in IET Electrical Systems in Transportation ISSN 2042-9738

Year: 2019
Pages: 1 – 12
DOI: 10.1049/iet-est.2019.0021

Fuel Cell Vehicle Energy Management Strategy Based on Cost of Ownership

Kevin Davis [1*], John G. Hayes [2]

[1] Department of Process Energy and Transport Engineering, Cork Institute of Technology, Cork, Ireland
[2] Power Electronics Research Laboratory, School of Engineering, University College Cork, Cork, Ireland
[*]kevin.davis@cit.ie

Abstract: The paper presents a novel energy management strategy (EMS) which outperforms the published strategies developed for an international technology challenge, *IEEE Vehicular Technology Society (VTS) Motor Vehicles Challenge 2017*. The objective of the strategy is to minimise the cost of ownership of a low-power (15 kW) fuel cell-battery electric vehicle. Both the fuel consumption cost and power sources degradation costs are combined to represent the total cost of ownership. The simple adaptive rule-based strategy optimises the fuel cell (FC) operation during low-traction power operation and switches to battery charge-sustaining operation for high traction power operation. This minimises fuel consumption and increases the lifetime of the fuel cell and the battery. The strategy is then compared with the EMS of the 2015 Toyota Mirai, and the challenge vehicle model is modified to capture the learnings from the Mirai. Finally, a cost-benefit analysis for a plug-in fuel cell vehicle (PFCV) is considered in order to improve FC lifetimes and reduce costs for short drive cycles.

1. Introduction

The objective of this paper is to develop an optimised rules-based EMS for the FCV model shown in Fig. 1 which was provided in the *IEEE VTS Motor Vehicles Challenge 2017* [1], while also modifying the model based on the 2015 Toyota Mirai FCV, and considering a plug-in FCV option. This was the first VTS challenge to develop an EMS for a FCV within a limited development time and 48 participants from 14 countries each developed an EMS. The second VTS challenge (2018) required the development of an EMS for a plug-in hybrid electric vehicle (PHEV), while the 2019 challenge involves an EMS for a locomotive application.

Fuel cell vehicles (FCV) are hybrid-electric vehicles (HEV) with a FC as the primary power source for the traction drive [2,3]. The FC is a low-voltage source and requires a boost converter at the FC output to increase the dc link voltage at the input to the traction drive, thereby reducing the inverter and motor losses in the traction drive system [4]. The FC is a unidirectional power source, and so requires secondary power sources, such as batteries and supercapacitors, to absorb regenerative braking energy [5]. The dynamic response of a FC has, until recently, been regarded as slow which has resulted in these secondary power sources providing power to the traction motor during vehicle acceleration to improve the performance of the vehicle [6-8].

An EMS controls the power sharing between the primary and secondary power sources in the FCV. The complexity of the EMS and the controllability of each power source depends on the configuration of the power sources in the FCV. The simplest configuration, shown in Fig. 1, uses a battery or supercapacitor directly connected to the boost converter output. In this configuration, battery power equates to the difference between the traction power and the FC output power. The EMS can directly control the FC power output while also indirectly controlling the battery power during steady-state operation. If the dynamic power response of the FC is limited, the EMS typically provides the average traction power requirement while minimising hydrogen (H_2) fuel consumption by optimising the operating point of the FC [9]. Note that a bidirectional dc-dc typically interfaces the battery to the dc link in high-power vehicles such as the Toyota Mirai [10].

The price premium associated with new zero-carbon emission vehicles such as an FCV, can be a barrier to their adoption by consumers. Research studies show that if a total cost of ownership (COO) approach is applied to these vehicles, then the lower fuel costs [11,12] or the higher resale values [13] can offset the purchase price premium during the initial years of ownership (typically a three-year period). Life-cycle-cost analysis studies [14] are conducted over a longer time period and in these studies, the degradation of a major power source such as the battery or the FC, can result in high replacement costs. These replacement costs can negate the lower fuel costs in the initial years of operation. Development of an EMS in a HEV design, using an internal combustion engine (ICE) as the primary power source, tends to focus on minimizing fuel consumption but the significance of power-source replacement costs to the real operating costs of these vehicles is rarely mentioned. Given that a FC vehicle has two power sources with degradation rates higher than the ICE of a conventional vehicle, minimising the degradation rates must be a critical operating strategy for this vehicle. This leads to the concept of developing an EMS based on minimising COO costs rather than just minimising fuel consumption.

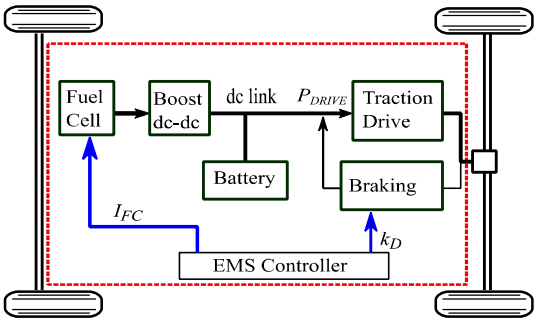

Fig. 1. *FCV model configuration for the VTS challenge*

The 2017 challenge scoring was based on the total COO, which comprise the combined costs associated with H_2 fuel consumption, FC degradation, battery degradation as well as a battery recharge cost to restore the battery to 100% state of charge (*SOC*) at the end of each drive cycle. The EMS can only control the FC output current, I_{FC}, within a range of 0 to 400A, and the regenerative-braking distribution factor, k_D, within a specified range of 0 to 0.5. All the costs in this paper are reported in US dollars ($) as this was the currency required in the challenge.

This paper presents an optimised rules-based EMS for the challenge model which outperforms the published strategies for this challenge. The authors provide an overview of EMS development techniques and power source degradation mechanisms. The EMS of the Toyota Mirai is explored based on the Argonne National Laboratory (ANL) test report [8]. The challenge vehicle model is modified to match the Mirai FC performance. Finally, a PFCV is considered as a viable option to reduce drive cycle costs and increase the FC lifetime.

The paper is organised as follows; EMS development techniques, FC degradation and battery degradation are reviewed in Section 2. Section 3 details the FCV model provided in the challenge. Section 4 describes the experimental tests and offline-optimisations to develop our EMS. Section 5 presents the Simulink model of the new simple adaptive rule-based EMS. Section 6 examines the 2015 Toyota Mirai and the modifications to the challenge FCV model. Section 7 is a cost-analysis of a PFCV configuration to reduce the total ownership costs for short drive cycles. Section 8 provides some concluding remarks.

2. EMS and Power Source Degradation

This section reviews the literature on EMS development in HEV designs and on operating conditions that impact degradation in both FC and batteries. A brief review of other studies on EMS for FCV is also included.

2.1. EMS Development Techniques

The objective of an EMS is to specify the operating levels for each of the power sources in a HEV or FCV to minimise a particular quantity, e.g. the fuel consumption of the vehicle over a given drive cycle. The system optimisation problem is usually specified with numerous system constraints such as the dynamic operational limits of individual system components. The techniques used to solve this problem may be classified as model-based optimisation or rule-based optimisation.

Model-based optimisation tends to be computationally complex and requires long computational times. Model-based techniques are difficult to implement for real-time control of power sources as they also require prior knowledge of the complete drive cycle to determine an optimum global solution. The most frequently referenced model-based optimisation techniques are Dynamic Programming (DP), Pontryagins Minimum Principle (PMP), and Equivalent Consumption Minimisation Strategies (ECMS) [15-17].

DP yields an optimised global-solution for a cost function provided the time horizon of the problem is fixed, and provided that simple mathematical models of the system can be formulated [18]. The optimised solution is found by defining possible system states for each time-period interval within local and global system constraints. Starting at the final system state, the costs associated with transitioning between all possible states in a time interval to all possible states in the previous time interval are calculated. This reverse-time calculation method is repeated until the costs of transiting from all the previous possible states to the current state are calculated. By determining the sum of all possible path costs from the starting interval state to the final interval state, it is then possible to determine the operating state at each interval, which results in the minimum overall path costs. As the DP technique has prior knowledge of the complete drive cycle, it can provide a global optimised solution. This solution may be used to benchmark less computationally-intensive, real-time control strategies over the same drive cycle. PMP is a numerical solution method that also determines an optimal global solution using an iterative technique, called the shooting method. PMP is described in Chapter 5 of [18].

ECMS is a computationally less intensive technique which determines local, rather than global, optimisation solutions. When the objective of the EMS is to minimise fuel consumption, the ECMS process assigns a fuel consumption value to the power associated with each source in the HEV. For a primary source, the efficiency map of the power converter (ICE or FC) will determine the fuel consumption. For a secondary source, such as the battery, the electrical power must be converted to equivalent fuel-flow rates using equivalence factors. The main challenge with ECMS is the selection of these equivalence factors as they will vary with power-flow direction (charge or discharge), with the efficiencies of components in the power path, and with the source of the charge power (primary source or regenerative braking). Ideally, they can only be optimised if the future driving conditions are known; for example, if in some future part of the drive cycle, significant regenerative braking energy is

available, then using electrical energy now will have little impact on fuel consumption because this electrical energy will not be replenished by the primary source fuel.

Simpler EMS techniques involve the development of rules to govern the source power levels. These rules can be based on: (i) heuristics or engineering experience, (ii) offline-optimisation of individual components (local minima) to determine maximum component efficiency conditions, and (iii) optimisation of the complete vehicle system in a defined state, e.g. braking, battery-charging, high-acceleration, urban-driving or highway-driving. The success of a rule-based EMS depends on many factors including the level of engineering expertise available, the accuracy of the component models, the ability of the EMS to quickly identify the operating state based on the available feedback signals, and the ability to convert expertise into rules using techniques such as fuzzy logic controllers (FLC) [19].

2.2. Review of EMS Development for FCV

EMS development for FC vehicles is a recent field of study and existing literature is limited in scope. The literature focuses on FCV EMS development which minimises fuel consumption and maximises the range. In this paper, minimising the COO is the objective of the EMS and this requires a study of the literature for the causes of degradation in both power sources.

Optimisation using model-based techniques for real-time applications has led some researchers to overcome the requirement for prior knowledge, by initially optimising using multiple sets of the legislative drive cycles. The resulting optimised strategies are then correlated to specific driving characteristics, e.g. urban driving (low speed with frequent stop-starts), highway driving (constant high-speed), or aggressive driving (high speed with rapid acceleration and deceleration). Real-time control can then be achieved as the EMS selects an optimised control set based on the current driving characteristics. The control-set selection can be achieved using lookup tables, fuzzy logic or simple rule-based controllers. This technique was applied in EMS development for the Chevy Volt PHEV [20] and achieved the minimum fuel consumption in the 2018 VTS challenge. Optimised control sets for a FCV, developed using DP, are presented in [21].

Other studies that implement model-based optimisation techniques include [22], where PMP is applied to a series-HEV to minimise fuel consumption, and the computational time is reduced by utilising probability distributions for future traction demands. In [23], minimisation of the fuel consumption and battery degradation are the dual objectives which are resolved using PMP for a parallel-HEV. The PMP is implemented online using an ECMS and the results indicate that to maximise the battery lifetime, the SOC range must be limited. As shown in [24], prioritising the battery-lifetime leads to a load-following strategy for the FC.

Rule-based strategies are more widely implemented than model-based strategies in the literature. A review of the ten best scoring EMS in the 2017 VTS challenge, shows that most utilise rule-based strategies [25] and achieved optimised results similar to the benchmark DP model-based strategy developed by the challenge organisers. Using DP, the optimal COO result for the 32.6 km challenge drive cycle is $1.612. The winner of the challenge [26] achieves a trip cost of $1.624 using a rule-based battery charge-sustaining (CS) strategy implemented using a simple proportional-integral (PI) loop controller. The challenge runner-up also implemented a rule-based CS strategy with the FC current specified using one of seven FC operating states [21]. These operating states are defined by the SOC and the traction power. The third-place finisher uses a look-up table (LUT), which is indexed by the traction power and the actual SOC [27]. The LUT values are established by offline optimisation of the total cost equations specified in [1] and assume steady-state operation, with the FC polarisation curve approximated as a linear function of FC current. This cost optimisation identifies elliptical power-sharing relationships between the two power sources, dependent on traction power and SOC. While this real-time optimisation method specifies the FC operating output once the FC switches on, it does not specify the optimum FC switch-on criteria. Battery-only operation, for the initial part of the challenge drive cycle, results in a total cost of $1.647 for this EMS. The authors of this paper also contributed an EMS to the challenge and achieved a fifth-place finish, with a total trip cost of $1.656. Our EMS was also rule-based with some offline-optimisation of the FC (combined H_2 consumption, FC degradation and dc-dc converter efficiency). As with the EMS presented in [27], our EMS has a FC switch-on at 70% SOC but this results in overall higher battery degradation costs, based on the model.

Other rule-based strategies for FC vehicles include a research study by Yue et al. [28] who developed an EMS that controls the FC output and reduces the degradation of the battery. They employ a FLC that uses thirty-six rules to set the FC current to one of nine possible levels. The input parameters are traction demand, battery SOC and battery remaining useful life, which has been estimated using prognostics. This EMS achieves a 4.75% reduction in battery degradation but does not specify the change in FC fuel economy or the impact on FC degradation to achieve this reduction. Hames et al [9] tested four fuel-saving control strategies in a FCV with both battery and supercapacitor (SCAP) secondary power sources. While their strategies incorporated both battery and SCAP min\max SOC values as constraints, the level of power source degradation is not evaluated. An ECMS is proposed as the optimum strategy based solely on achieving the minimum hydrogen consumption over a given drive cycle. Two control strategies for a FCV are presented in [29]: one to minimise fuel consumption by maximising the utilisation of the battery and SCAP power sources; the other for reduced battery degradation by utilising the SCAP to supply the high-current pulses to the traction drive and to receive high-current pulses during regenerative braking. While the latter strategy in [29] lowers battery degradation, the impact of each control strategy on FC degradation is not presented in their paper. In stop-go driving conditions, their study demonstrated that H_2 consumption increases significantly (173%) when the reduced battery degradation strategy is employed. An adaptive FLC EMS is proposed for a low-power FCV in [30] and focuses on optimising the powertrain control rather than utilising a fuel minimisation strategy. This EMS adapts to three load conditions (braking, normal driving and max power driving) by adjusting the FC power output and the FC dynamic-response rate for load changes to maintain the battery SOC at a reference value.

2.3. Power Source 1 - FC Degradation

An understanding of the root causes of FC degradation during normal vehicle operating conditions is necessary in order to optimise the durability of a FC. FC operation is usually explained as a steady-state energy conversion process where hydrogen is provided to the anode and oxygen (O_2) to the cathode. At suitable temperatures, the hydrogen splits into hydrogen ions, which migrate to the cathode via a membrane, and into electrons which flow in an external circuit. Waste water results when the hydrogen ions react with the O_2 at the cathode. The output power is determined by controlling the flow rates of each gas based on the stoichiometric ratio for this reaction. The balance of plant (BOP) controls the steady-state gas flow requirements and the removal of waste water. In steady-state benign conditions, FC stack lifetimes of more than 25,000 hours are possible [31].

Under dynamic conditions, such as found in vehicle applications, process control is considerably more complex. As the power demand varies, the BOP must quickly adjust the gas flow rates to match the new power demand. An additional vehicle FC issue is that air needs to be pumped to meet the O_2 requirement at the cathode. Under high-power conditions, the BOP must be designed to flow a high volume of air to the cathode. A study by Pei et al. [31] summarises four vehicle operating conditions which may result in FC degradation, namely, load-cycling operation, stop-start operation, high-power operation and low current operation (idling). Accelerated lifetime testing of a FC stack from a bus [32] showed that 56% of the FC degradation was due to load-cycling and 33% due to stop-start operating. This study derived performance deterioration rates of 0.0000593 % per cycle for large-range load-cycling, 0.00196 % per cycle for stop-start cycling, 0.00126 % per hour for idling operation time and 0.00147 % per hour for high-power operation. The reduced FC lifetime, when operating under such dynamic conditions, can be as low as one-tenth of the lifetime under steady-state conditions.

Studies of FC degradation in vehicles [33-35] show that the principal FC stack degradation mechanisms are membrane dehydration and incorrect stoichiometric ratios due to flooding in the gas flow channels. For example, during idling operation, the maintaining of membrane hydration is difficult due to the low levels of waste water available, and so micro-cracks may form on the dehydrated membrane. During high-power operation, waste-water flooding in the air channels can cause non-uniform power generation and lead to excessive temperatures within the stack. The degradation found under stop-start conditions results from incorrect gas conditions at one, or at both electrodes. When the FC has been off for a time, air from the cathode side can migrate to the anode side. At start-up, the FC open-circuit voltage can only be developed when the H_2 fuel has displaced any leaked air at the anode. In the absence of H ions, O_2 in the air oxidises with the carbon structure which supports the platinum catalyst particles at the cathode. Carbon dioxide (CO_2) or carbon monoxide (CO) is formed and the catalyst is lost as its carbon structure degrades. A similar condition can occur when the H_2 fuel flow is shut off. The greatest challenge for the BOP equipment for load-cycling conditions is maintaining the humidity at both the anode and the cathode sides of the membrane while simultaneously controlling the stack temperature. The high number of these cycles during vehicle operation can result in a significant deterioration of the stack output voltage within a relatively short period of time (1000-3000 h), despite the fact that degradation associated with each individual load cycle is low. FC degradation due to air pollutants and to waste-water freezing in cold ambient temperatures, can be minimised by good BOP design.

2.4. Power Source 2 - Battery Degradation

Modelling of battery degradation is achieved using physically-based electrochemical models which require detailed information about the internal chemical construction or by using semi-empirical or empirical models that establish degradation relationships using experimental test data. The complex electrochemical models have been shown to provide the best degradation estimates [36], but the simpler empirical models are easier to integrate into vehicle simulators and are used in this study. The two battery types used in FCV are Nickel Metal-Hydride (NiMH) and Lithium-ion (Li-ion). As Li-ion is the dominant battery technology in vehicles, this paper will review degradation mechanisms in this battery type, although the 2015 Toyota Mirai FCV features a NiMH battery. Battery degradation is associated with a loss of usable capacity (capacity fade) and with an associated increase in the internal series resistance which restricts the power output (power fade) of the battery.

Battery degradation can be classified as either calendar degradation or as cycle degradation. Calendar degradation refers to the loss of capacity over time when the battery is neither charging nor discharging. Ambient temperature is the main impact factor in calendar degradation across all battery chemistries and the degradation rate is modelled using a power law relationship known as the Arrhenius equation. The equation states that degradation rates increase as ambient (battery) temperatures increase and is valid for Li-ion chemistries. It is not applied to sub-zero ambient temperatures applications as the electrochemical degradation mechanism for Li-ion is different at these temperatures [37]. The general form of this Arrhenius equation for battery degradation, is given as

$$Q_{LOSS\_CAL} = A_{CAL} e^{\left(-E_A/RT\right)} t^X \tag{1}$$

where $Q_{LOSS\text{-}CAL}$ is the percentage battery capacity loss, A_{CAL} is a curve-fitting coefficient determined using test data, E_A is the battery cell activation energy (J/mol), R is the universal gas constant, T is the ambient temperature (K), t is the test time period which is usually specified in days due to the long-time constant associated with calendar degradation and x is the power law value which is commonly assigned a value of 0.5 [38]. In addition to temperature, the rate for calendar degradation is dependent on the battery SOC. For Li-ion batteries, increased calendar degradation occurs at very high (SOC>80 %) values of SOC [39].

Cycle degradation rate is impacted by multiple operational parameters of the application. Examples of impact factors include depth of discharge (DOD), charge and discharge capacity (C) rate, ambient temperature and the number of load cycles.

Cycle degradation can be compared to mechanical fatigue modelling [40] and it is difficult to establish individual parameter impacts on the degradation rate as the impact parameters are interlinked. One approach to simplify cycle degradation modelling [38, 41] is to combine the DOD and cycle-number parameters into a single Ampere-hour (Ah) throughput value and then to use regression analysis to relate the temperature and *C* rate to experimental test data. This yields an empirical model for percentage capacity loss in the form of

$$Q_{LOSS-CYC} = \left(aT^2 + bT + c\right)e^{\left[(dT+e)C_{RATE}\right]}Ah + ft^{0.5}e^{\left(-E_A/RT\right)} \tag{2}$$

where *a,b,c,d,e,f* are the coefficients fitted to the test data. The validity of this approach is questionable as the Ah throughput of a battery is not constant but is a quadratic function of DOD [42]. In [43] an effective Ah throughput is determined using severity maps. The severity map provides a degradation rate for each set of conditions (SOC, temperature, magnitude of current) in a given cycle and integrating these rates over time, provides an effective Ah value. The complexity in modelling cycle degradation is further demonstrated by a study in Sweden [44], where the impact of battery current direction (charge or discharge) was tested and the cycle degradation is found to be higher when charging at high *C* rates compared to the equivalent degradation recorded when discharging at the same *C* rate. Alternative cycle degradation models for Li-ion batteries which are based on loss of active material or SEI layer growth are discussed in [36].

The increase in battery series resistance, which results in power-fade, is modelled in [45] as

$$R_{SERIES}\left(soc\right) = a_0 e^{\left(-a_1 SOC\right)} + R_{INIT} \tag{3}$$

where a_0, a_1 are test data coefficients and R_{INIT} is the initial measured series resistance of a fully charged battery. This model results in a rapid increase in resistance as the SOC drops below 20%. Combining this model with the impact of high SOC on calendar degradation found in [39], minimum battery degradation occurs when the SOC is constrained in a range from 20% to 80%.

3. Fuel Cell Vehicle Model

The challenge vehicle parameters are presented in Table 1. The equations of the FCV model are either published in [1], or else extracted by the authors from the Matlab\Simulink model provided by the challenge organisers. The vehicle specification is based on the 2009 model of the Tazzari-Zero EV [46], a low-cost commercial FCV.

Table 1 Vehicle model parameters [1]

Parameter	Symbols	Units	Value
Max traction power		kW	15
Max traction force		Nm	2000
Vehicle mass	*m*	kg	698
Wheel radius		m	0.2865
Gear ratio			5.84
Frontal area	A_F	m^2	1.942
Drag coefficient	C_D		0.36
Rolling Resistance	C_{RR}		0.02
Fuel cell max power		kW	16
Fuel cell max current		A	400
Fuel cell max voltage		V	60
Fuel cell min voltage		V	40
Battery capacity	Q_{BAT}	Ah	40
Battery max voltage		V	100.8
Battery min voltage		V	60

The traction force (F_T) is based on the vehicle speed and the acceleration requirements of the drive cycle

$$F_T = mgC_{RR} + 0.5\rho C_D A_F v^2 + mg\sin\alpha + ma \tag{4}$$

where the parameters are vehicle mass *m* (kg), frontal area A_F (m^2), drag coefficient C_D, tire rolling-resistance coefficient C_{RR}, vehicle acceleration *a* (m/s^2), air density ρ (1.223 kg/m^3), gravity *g* (9.81 m/s^2), road grade α, and the net relative air velocity *v* (m/s) which is the combined vehicle and wind velocities. The regenerative braking distribution force, k_D, is a fraction of this traction force and it is limited to a maximum of k_D=0.5 in this front-wheel drive vehicle (k_D=0 represents no regenerative braking available).

The COO costs per drive cycle are calculated based on the fuel and the power source replacement costs presented in Table 2. These costs are based on US Department of Energy system target costs for 2020.

Table 2 Fuel costs and component replacement costs [1]

Parameter		Units	Value
FC replacement cost	FC_{cost}	$	600
Battery replacement cost	BAT_{cost}	$	640
H_2 fuel cost	$H2_{cost}$	$/g	0.0035

The H_2 mass flow rate ($\dot{m}_{H2}$) with units (g/s), is given as a linear equation:

$$\dot{m}_{H2} = \left[a\left(I_{FC}\right) + b \right] \times 0.08988 / 60 \tag{5}$$

where a and b are the experimentally validated coefficients of the FC model, as shown in Table 3, and I_{FC} is the FC output current. The FC output voltage, V_{FC}, is modelled using a polynomial relationship to FC output current:

$$V_{FC} = c(I_{FC})^3 + d(I_{FC})^2 + e(I_{FC}) + f \tag{6}$$

where c, d, e and f are the FC coefficients shown in Table 3.

Table 3 FC model coefficients [1]

Coefficient	Value
a	0.52488
b	15.835
c	-6.7791e-07
d	0.00044927
e	-0.11913
f	59.124

The dc-dc boost converter efficiency (η_{BOOST}) is given as:

$$\eta_{BOOST} = \left[-0.0095\left(I_{FC}\right) + 95 \right] \tag{7}$$

The degradation of the FC (Δ_{FC}) at time t is a combination of the number of start-stop events N_{SWITCH} and a quadratic function of the operational power of the FC:

$$\Delta_{FC}\left(t\right) = \Delta_{SWITCH} N_{SWITCH} + \int_0^t \delta\left(t\right) \tag{8}$$

where the operating-power degradation function is:

$$\delta\left(t\right) = \frac{\delta_0}{3600}\left(1 + \frac{\alpha}{P_{FC-NOM}^2}\left[P_{FC}\left(t\right) - P_{FC-NOM} \right]^2 \right) \tag{9}$$

Parameter Δ_{SWITCH} is a start-stop event FC degradation coefficient, δ_0 and α are FC operating-power degradation coefficients, and all of the coefficient values are provided in Table 4. Parameter $P_{FC\text{-}NOM}$ is the nominal power of the FC, which has a specified value of 6 kW for this FCV.

Table 4 FC degradation coefficients [1]

Coefficient	Value
Δ_{SWITCH}	$2.5\text{x}10^{-4}$
δ_0	$0.5\text{x}10^{-4}$
α	4

FC degradation has a significant impact on the EMS development and is high for drive cycles with frequent FC start-stop events due to the high value of Δ_{SWITCH}. This FC degradation model captures two of the four vehicle operating conditions [31] reported

in the literature. The impact of load-cycling and idling are not represented in the model equations. Load-cycling is severely restricted by the slow dynamic response of the FC model to avoid this degradation condition.

Battery degradation (Δ_{BAT}) is determined using the magnitude of the battery current (I_{BAT}), SOC and the battery operational state, e.g. discharging ($I_{BAT}>0$) or charging ($I_{BAT}<0$). The battery degradation at time t is given as

$$\Delta_{BAT}(t) = (1/Q_{LIFETIME}) \int_0^t \left| F(soc)\, G(I_{BAT})\, I_{BAT} \right| dt \tag{10}$$

where

$$F(soc) = 1 + 3.25(1 - SOC)^2 \tag{11}$$

Parameter $Q_{LIFETIME}$ is the effective battery throughput [43] in ampere-seconds, calculated using the nominal battery capacity Q_{BAT} of 40 Ah:

$$Q_{LIFETIME} = 15000 \times 3600 \times Q_{BAT} \tag{12}$$

The degradation component $G(I_{BAT})$ is dependent on the battery current and is determined using

for $I_{BAT} > 0$

$$G(I_{BAT}) = 1 + 0.45(I_{BAT} / I_{RATED}) \tag{13}$$

for $I_{BAT} < 0$

$$G(I_{BAT}) = 1 + 0.55(I_{BAT} / I_{RATED}) \tag{14}$$

where I_{RATED} is the rated current of the battery (40A for this vehicle). The ratio I_{BAT} / I_{RATED} is the C rated value of the battery current. While the literature identifies temperature as a major battery degradation factor for both calendar and cycle degradation, it is not included in this model. Also, analysis of these two degradation model functions (Fig. 2) shows a linear increase with C rate and a power law relationship with SOC, with minimum degradation occurring at 100% SOC. This SOC-degradation function conflicts with the literature, which shows a high SOC can lead to a high level of degradation [39]. In this vehicle model, operating the battery near to 100% SOC will reduce battery degradation costs. This degradation function, when combined with a challenge constraint which specified 100% SOC at the end of each drive cycle, greatly influenced the development of an EMS for this vehicle. However, this topic is revisited in Section 6.

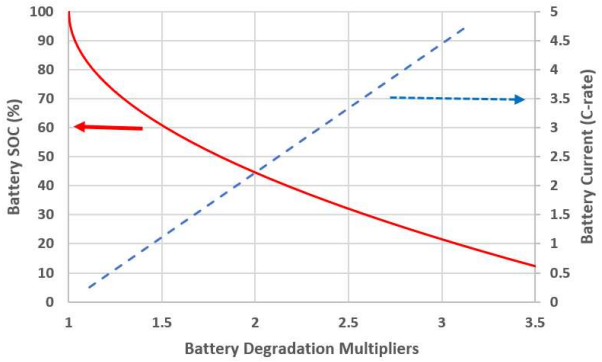

Fig. 2. *Battery Degradation*

The model recharges the battery using the FC. The recharging cost ($\$_{CHG}$) is calculated for the additional H_2 required, FC degradation, boost efficiency and battery degradation during the recharge operation. FC degradation costs are higher if the FC is off at the end of the drive cycle and must be switched-on again to meet the battery recharge requirement. The vehicle model provides two equations to calculate the recharging costs dependent on the FC status (on or off) and the final battery SOC (SOC_F) at the end of the drive cycle:

FC on:

$$\$_{CHG} = -0.0286\left(SOC_F\right)^3 + 0.2527\left(SOC_F\right)^2 - 1.362\left(SOC_F\right) + 1.1376 \quad (15)$$

FC off:

$$\$_{CHG} = -1.7987\left(SOC_F\right)^3 + 2.9842\left(SOC_F\right)^2 - 2.6188\left(SOC_F\right) + 1.4543 \quad (16)$$

Total drive cycle costs ($\$_{TOT}$) are calculated by converting the degradation values to costs using the component replacement costs in Table 2. These costs are then summed with the fuel costs and recharging costs.

$$\$_{TOT} = FC_{COST}\Delta_{FC} + BAT_{COST}\Delta_{BAT} + H2_{COST}\int_0^t \dot{m}_{H2}dt + \$_{CHG} \quad (17)$$

The FC model's dynamic response uses three rate-limiting components connected in series; a 6 A/s current rise limit (FC output currents < 150 A), a 20 A/s current rise limit (FC output currents >150 A) and a 15 mHz low-pass filter. The significance of this slow FC dynamic response for EMS development is presented in Section 4.

4. EMS Development Strategy

The competition organisers provided the vehicle model with a simple rule-based EMS (referred to as the baseline-EMS in this paper), which implements thermostat-type control of the FC. The FC starts when the battery SOC drops to 40% and operates at the maximum power output until the FC stops at an SOC of 70%. The initial braking strategy sets k_D to zero, which implies no regenerative braking. Three drive cycles are provided as part of the vehicle simulation model. Two drive cycles are adapted versions (max. speed restricted to 85 kmph) of legislative vehicle test cycles: New European Drive cycle (NEDC) and the class 2 version of the Worldwide-harmonised Light-vehicle Test Cycle (WLTC). A third drive cycle (Urban) is based on a short (380 s) recorded journey by the University of Lille in a Tazzari-Zero vehicle. The challenge organisers used a fourth drive cycle (referred to as *VTS*TC in this paper), with a 2590 s duration, to score any EMS developed by the 2017 challenge participants.

As the duration of the challenge drive cycle is unknown, model-based optimisation techniques such as DP and PMP could not be implemented for EMS development. Instead the approach followed is similar to ECMS, except that equivalent costs rather than equivalent fuel consumption are modelled. Each power source, FC and battery, was analysed in terms of the costs to provide 1 kWh to the input of the traction drive on the dc link.

The cost map ($/kWh) for the FC is developed using Matlab arrays as follows: a FC power-output relationship with I_{FC} is established when (6) is multiplied by a 0-400 A range of I_{FC} values. Equation (5) establishes the H_2 consumption at each power level, which can then be normalised to a fuel cost per kW at the FC output. FC degradation costs for each power level (neglecting the FC start-stop degradation costs) can be calculated using (9) and combined with the fuel costs. The boost converter efficiency (7) is applied to the combined costs at the FC output terminals in order to determine the cost per kWh at the dc link,. These calculations are summarised in a FC cost map at various I_{FC} values in Fig. 3. The optimised FC operating power level is impacted by both the boost converter efficiency and the FC degradation. When only fuel costs are considered, the optimised FC operating-level is at 244 A (11.46 kW) with a resulting cost per kWh of $0.237, shown as OPT 1 in Fig. 3. When the FC degradation costs are included, the optimum operating-level shifts down to 184 A (8.87 kW) and the cost rises to $0.249 /kWh, shown as OPT 2 in Fig. 3. Finally, when the boost converter efficiency is also considered, the optimum operating-level reduces further to 172 A (8.34 kW) and results in a cost of $0.263 /kWh, shown as OPT 3 in Fig. 3. This analysis identifies a single optimum point and also shows the low variation in FC costs (less than $0.01/kWh) in the I_{FC} range of 105 A (5.2 kW) to 275 A (12.5 kW), suggesting that a wide operating range is possible for the FC without incurring significant COO costs. The cost associated with FC degradation for each stop-start event is calculated using the FC replacement cost (Table 2) and the degradation coefficient Δ_{SWITCH} (Table 3). The high cost of $0.15 per event advocates that the developed EMS must minimise the number of FC start-stop events in each drive cycle.

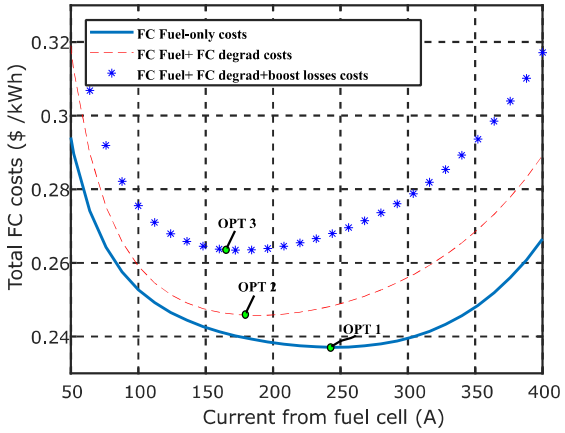

Fig. 3. *FC offline-optimisation to provide 1 kWh at dc link*

In this FCV, the battery energy can only be recharged by the FC or by regenerative braking. For FC-supplied battery energy, the total costs for the battery to resupply 1 kWh of this stored energy back to the dc link, would be the combination of the recharge cost plus the discharge costs. The recharge cost is the sum of the previously calculated FC costs, internal energy loss in the series resistance, and the battery degradation costs during recharging. The discharge cost is the combined series-resistance energy loss costs and the battery degradation costs during discharge. As the battery degradation costs are dependent on both the SOC and the battery current direction (charging or discharging), a cost map for the battery has many dimensions which also depend on the rates of charging and discharging. In order to simplify the cost calculation, the same current value is assumed for both charge and discharge battery currents. Using equations (10-14), a cost-map for 1 kWh provided by the battery at the dc link is shown in Fig. 4.

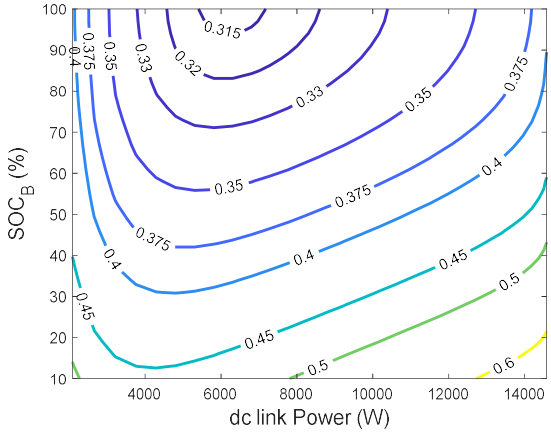

Fig. 4. *Battery offline-optimisation per kWh at dc link*

The map shows that battery operation at low SOC levels results in higher costs. When Fig. 4 is compared to Fig. 3 it is apparent that battery-only operation for this FCV would result in significantly higher COO costs than FC-only operation. This cost map also identifies the FC output power required to minimise the recharging costs based on the battery SOC value.

Assuming steady-state operation, the offline equivalent-cost optimisation of the power sources (Fig. 3 and 4) suggests that FC-only operation should achieve minimum drive cycle costs. An EMS to achieve FC-only operation is a load-following strategy where the traction power demand at the dc link, P_{DRIVE} (shown in Fig.1), is converted to a FC current demand I_{FC}. This type of load-following strategy is possible with some advanced designs of FCV, such as the Toyota Mirai [7]. However, the dynamic response of the FC stack in the challenge vehicle, is considerably slower than the dynamic power rates required by the traction drive.

Optimisation which includes component dynamic performance constraints is beyond the scope of this study, but experimentation using the Matlab-Simulink model provided useful insights into what might be achieved. For example, when a simple load-following EMS was developed for the FCV, the results in Fig. 5 show that the FC is unable to track the traction power requirement. As the challenge did not allow participants to change the dynamic response, battery operation is required for the vehicle during acceleration and braking in each drive cycle. As the battery is directly connected to the dc link, an EMS has only limited control on the instantaneous battery power (and current) levels. Fig. 5 also clarifies that the traction power

requirements during acceleration are higher than the 16 kW available from the FC which also leads to a battery power requirement for peak traction loads.

Further experimentation with the vehicle model illustrates that the required traction energy, measured at the input of the traction drive (P_{DRIVE}), is independent of the battery voltage value. With full regenerative braking (k_D=0.5), the traction energy requirement at the dc link is 2% lower for the NEDC and WLTC drives cycles, and is 11% lower on the Urban drive cycle. Using the baseline-EMS, model simulations show that the degradation costs for one FC start-stop event represents up to 24% of the COO costs for an Urban drive cycle.

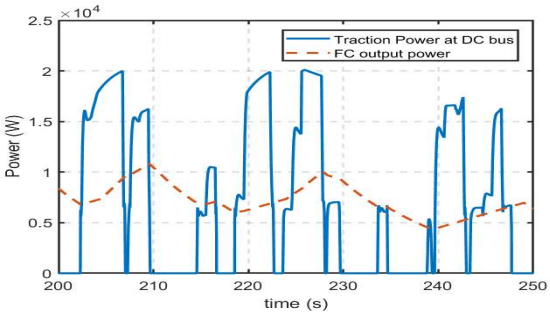

Fig. 5. *FC dynamic response using load-following EMS*

The combination of the equivalent-cost analysis of the power sources and the experimentation with the vehicle model resulted in a set of optimising vehicle operating conditions which were used to develop a rule-based EMS. These conditions are as follows:

(i) Minimise the FC start-stop events per drive cycle to one event.
(ii) Maintain the battery SOC close to 100 % while ensuring the FC is not turned off (FC is turned off if the battery SOC reaches 100% or the FC output current drops below 10mA).
(iii) Operate the FC close to its optimum power level for minimum COO costs ($P_{FC\text{-}OPT3}$ =8.34 kW or $I_{FC\text{-}OPT3}$ =172 A).
(iv) Reduce the traction energy requirement for H_2 fuel by maximising the recovered energy using a high regenerative braking distribution factor, k_D=0.5.
(v) Prioritise FC output over battery output for increasing traction power demands due to the lower equivalent costs associated with the FC power source.

In order to simultaneously meet the requirements of conditions (i) to (iv) with the slow power dynamics of a power plant, such as the FC, a safety margin must be incorporated into the EMS. Restricting the FC start-up until the battery SOC has dropped from 100% to 95% SOC provides a 5% SOC margin before the FC will be turned off again. Condition (i) can be achieved by linearly decreasing the FC power output as the battery approaches 100% so that FC turn-off conditions are not reached before the end of the drive cycle. A linearly-decreasing regenerative braking distribution factor k_D is applied when the battery SOC is higher than 98%. This prevents a regenerative braking event from recharging the battery to 100% which would result in the FC turning off. Condition (v) can be implemented by comparing the FC power output (P_{FC}) with the traction drive power P_{DRIVE}: if the P_{DRIVE} requirement increases, then P_{FC} is proportionally increased in response to the increasing traction demand. The EMS structure described can be implemented with the following six rules:

Rule 1: FC turned on when SOC<95%
Rule 2: SOC<95%, FC = $P_{FC\text{-}OPT3}$
Rule 3: SOC>95%, FC = k_P x $I_{FC\text{-}OPT3}$
Rule 4: SOC<95%, P_{DRIVE}> $P_{FC\text{-}OPT3}$, FC=(1+k_{sus}) x $I_{FC\text{-}OPT3}$
Rule 5: SOC<98%, k_D = 0.5
Rule 6: SOC>98%, k_D = k_R x 0.5
where k_P, k_{sus} and k_R are linearly decreasing proportional gains (equations supplied in Section 5).

5. Results for New Optimised Challenge EMS

The newly developed EMS, EMS-1 is shown in Fig. 6 and is a simplified version of the three previous EMS proposed by the authors for this vehicle [47]. The regenerative braking elements of the strategy (rules 5 and 6) are not shown in Fig. 6.

.

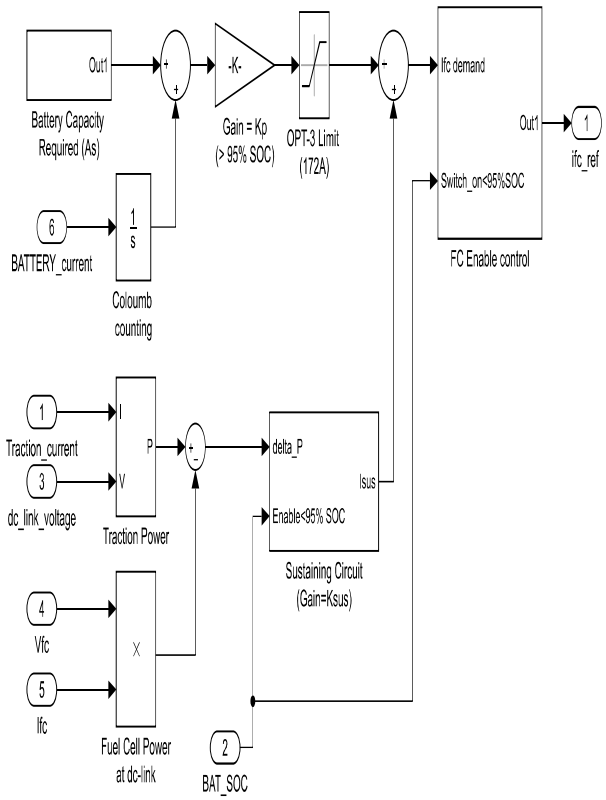

Fig. 6. *Simulink model implementation of EMS-1*

The FC current demand, *ifc_ref*, is zero until the FC is enabled. The FC turns on when the battery SOC drops to 95%. The battery recharging current demand is initially determined by converting the starting battery Ah value to an Ampere-second (As) value and this demand is updated each second using the Coulomb counting method as the vehicle completes the drive cycle. The maximum recharge current is set to the optimum FC current level of 172A. At 95 % SOC and above, a proportion gain (k_P) automatically reduces the current demand below the maximum as given by

$$k_P = 1/(0.05 \times 3600 \times Q_{BAT}) \tag{18}$$

If the battery SOC is below 95%, the FC will operate at its optimum power level of 8.34 kW (172A) and primarily supply the traction drive requirement, P_{DRIVE}. Any surplus power will recharge the battery. The remaining components in EMS-1 only become operational when P_{DRIVE} exceeds η_{BOOST} x 8.34 kW. In this condition, the FC power reaching the dc link is less than the traction drive power requirement, so the FC power is raised by calculating the power increase needed. This power increase is converted to a current-sustaining-demand value using a proportional gain (k_{SUS}) value given by;

$$k_{SUS} = (I_{FCMAX} - I_{FC-OPT3})/(P_{FCMAX} - P_{FC-OPT3}) \tag{19}$$

where I_{FCMAX} and P_{FCMAX} are the FC maximum current of 400A and power of 16 kW, respectively .

The regenerative braking strategy keeps k_D constant at 0.5 (Rule 5) and linearly reduces this factor using a proportional gain (k_R) when the battery SOC exceeds 98%.

$$k_R = 50(1 - SOC) \tag{20}$$

As per Rule 4, the sustaining circuit is only active while the SOC is less than 95%. The net effect of switching off the sustaining circuit and proportionally decreasing the battery recharge current demand, is that the charge-sustaining battery control keeps the SOC in the region of 97% (Fig. 7).

In the VTS challenge, the level of optimisation achieved by an EMS is evaluated by the minimisation of the COO costs over a drive cycle. For the *VTS*TC drive cycle, a benchmark cost of $1.612 was established by the challenge organisers using DP

optimisation. The proposed rule-based strategy, EMS-1, achieves a COO of $1.592 in the *VTS*TC drive cycle. This is a 2% improvement on the challenge winner costs of $1.624 and a 1% improvement on the benchmark DP optimisation costs.

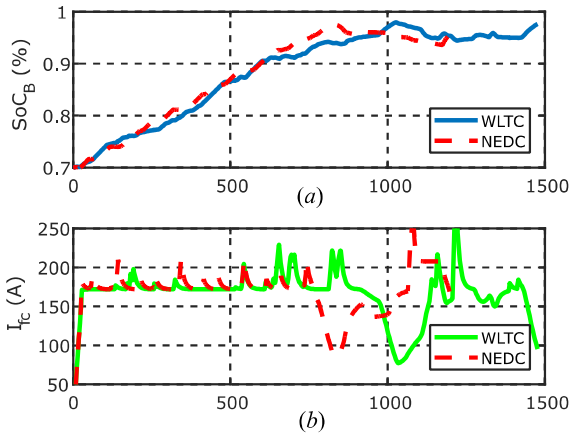

Fig. 7. (*a*) *SOC using EMS-1,* (*b*) I_{FC} *using EMS-1*

The proposed EMS was also evaluated for the three other drive cycles provided with the challenge model. A comparison with the baseline-EMS performance in terms of COO costs and the impact on power source lifetimes are detailed in Table 5. In these evaluations, the vehicle starts the drive cycle with a battery at an initial SOC of 70%. The impact of this starting condition is that each drive cycle will have fixed recharging costs associated with the challenge requirement that the battery must be fully recharged at the end of a drive cycle. The recharging fixed costs include the H_2 fuel costs, the FC degradation cost for a start-stop event, as well as FC and battery operational degradation costs. For each drive cycle the energy required at the traction drive input can also be regarded as a fixed cost as an EMS cannot change this traction energy demand. The approximated fixed cost for the traction energy in Table 5, is calculated by assuming P_{DRIVE} is to be provided only by the FC, operating at maximum efficiency ($0.2635 per kWh) and the battery discharge degradation costs are assumed to be zero.

Optimisation of the power sources using either model-based or rule-based EMS cannot achieve COO costs that are lower than the fixed drive cycle related costs. The results of simulations with the EMS-1 strategy show that COO costs are within 4% of these fixed costs. The EMS-1 strategy decreases COO costs by up to 29.5% when compared to the baseline-EMS for the WLTC drive cycle.

Table 5 Simulation results and fixed cost analysis

		Urban	NEDC	WLTC
DC bus Traction Energy	[Wh]	576	1610	2098
Min cost of Traction Energy	[$]	0.152	0.424	0.553
FC start-stop degradation cost	[$]	0.15	0.15	0.15
Battery recharge cost (70% SoC)		0.298	0.298	0.298
Total fixed drive cycle costs	[$]	***0.60***	***0.872***	***1.001***
Drive cycle costs(baseline-EMS)	[$]	0.74	1.09	1.46
Drive cycle costs (EMS-1)	[$]	0.625	0.897	1.029
Cost reduction using EMS-1		**15.5%**	**17.6%**	**29.5%**
FC lifetime (baseline-EMS)	[h]	N\A*	1104	1205
FC lifetime (EMS-1)	[h]	394	1196	1441
Battery lifetime(baseline-EMS)	[h]	1369	2532	1801
Battery lifetime (EMS-1)	[h]	2305	6031	6860

** FC not operating in this drive cycle using baseline-EMS*

Strategies can also be evaluated in terms of their impacts on power source lifetimes. EMS-1 improves the lifetime of both the FC and the battery. The FC operating times are shorter with the baseline-EMS but the higher power levels lead to higher levels of FC degradation and a lower FC lifetime. On the *VTS*TC, EMS-1 results in a FC lifetime of 2299 hours and a battery lifetime of 5465 hours. These are comparable to the DP optimised lifetime values of 2447 hours for the FC and 4703 hours for the battery.

6. Toyota Mirai Analysis and Model Modifications.

State-of-art mass produced FCV designs include the Honda FCX Clarity [48], the Toyota Mirai [49], and the Hyundai Nexo [50]. Their power-source ratings differ from many of the low-power FC vehicles tested in EMS development studies. The commercial FCV models are equipped with high power FC stacks (from 95 kW for the Nexo to 114 kW for the Mirai) to match the peak-power requirements of the vehicles. They also have advanced FC stack and BOP designs to improve gas flows and humidity controls, which result in higher dynamic power rates from the FC stack while significantly reducing the impacts of FC

degradation [51]. For cost reasons, FCV designs have the same powertrain configuration as existing high-volume HEV configurations, with the ICE and transmission system being replaced by a FC stack [52]. The EMS for these vehicles are not published in the literature but the basic rules of the operating strategy for the Toyota Mirai can be deduced from the tests carried out by ANL [8]. The condition for FC turn-on is when the DC bus power demand exceeds 5kW. During normal driving conditions, the EMS controls the FC with a load-following strategy. During braking and when idling, the FC is turned off. As Toyota offer an 8 year /100,000 miles warranty for the Mirai, their EMS suggests that they have significantly reduced the FC degradation impacts associated with load-cycling and start-stop events using new stack and BOP designs.

The FC system efficiency (the system includes the FC water pump, compressor, H_2 pump and the boost converter) has a peak efficient of 63.7% at low output powers (approx. 10 kW). This is consistent with vehicle power requirements for most drive cycles. FC degradation at high-power output is reduced by folding-back the peak FC power output after a period of approx. 30 s. The EMS maintains the battery SOC at a constant level of approx. 60%. This charge-sustaining level is consistent with the literature on battery degradation which identifies operating with a low-SOC (20%) or with a high-SOC (80%) as increasing the rate of battery degradation.

In this section, the FCV model is compared to the Mirai. The battery degradation equation (11) is replaced with an equation which is compatible with the Li-ion degradation mechanisms found in the literature and which reflects battery operation in typical HEV designs. The developed strategy, EMS-1, is modified to include the new battery degradation equation. The FC voltage and mass flow equations are modified to achieve the higher efficiency of the Toyota Mirai FC stack. This new FC model is tested with the EMS-1 strategy.

6.1. Charge-sustaining at 60% SOC

In order to optimise the COO over a drive cycle, the challenge FCV battery degradation model, as specified by (11), constrains EMS development to strategies with the battery operating at close to 100 % SOC. A proposed alternative degradation model is specified in equation (21) and is plotted with the original degradation model in Fig. 8.

$$F\left(SOC\right) = 0.98 + 7e^{(-10\,SOC)} + e^{\left[12(SOC-1.03)\right]} \tag{21}$$

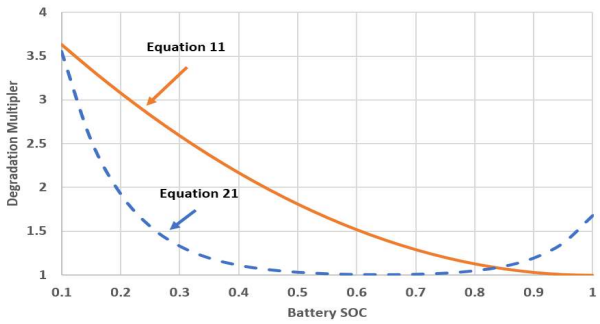

Fig. 8. *Battery degradation equation comparison*

This bathtub-curve-shaped model optimises battery operating in the range of 50 % to 80 % SOC. Modification of EMS-1 to minimise COO cost by applying this new battery degradation model involved changing; (i) FC turn-on from 95 % to 60 % SOC, (ii) sustaining circuit disable point from above 95 % SOC to above 60 % SOC, and (iii) the battery recharge current demand function to specify a linearly decreasing demand from optimum FC current to zero in the 5 % SOC region above the target SOC value (60 % in our tests). Implementation of these three parameter value changes achieved nearly identical *VTS*TC drive cycle combined costs for fuel, battery degradation and FC degradation as had been achieved when operating at a charge-sustaining level of 95 % SOC. The new COO cost for the *VTS*TC, without a recharge to 100 % requirement, was \$1.592 with an average battery SOC of 60 %, compared to \$1.586 for EMS-1 with an average battery SOC of 95%. The modified vehicle model allowed optimising strategies over a wider, more typical, range of battery SOC values.

6.2. Scaling the Mirai FC Stack

A scaled version of the Mirai FC stack is modelled by modifying equation (6) to reflect the improved current density of the Mirai FC [7] and the resulting FC polarisation curve is given by equation (22). The Toyota Mirai system efficiency test data in [8] can be used to derive a new FC mass flow equation (23).

$$V_{FC} = c - d\log_e\left(I_{FC}\right) - e\left(I_{FC}\right) \tag{22}$$

$$\dot{m}_{H2} = \left[a\left(I_{FC}\right)^2 + b\left(I_{FC}\right) + 2.7529 \right] \times 0.08988 / 60 \tag{23}$$

The new FC polarisation curve coefficient values and the mass flow coefficients are specified in Table 6.

Table 6 New FC model coefficients based on Toyota Mirai

Coefficient	Value
a	0.0005
b	0.4284
c	60
d	0.75
e	0.0172

Offline optimisation of the new FC model shows optimum FC efficiency occurs at 88A (4.87 kW). Using both the new FC model and incorporating the new optimum FC current into EMS-1, the combined costs for the *VTS*TC drive cycle were reduced from \$1.59 to \$1.19. The dynamic rate limits on the FC model had to be substantially increased to simulate the new model with the load-following strategy of the Mirai. The results for this strategy show a slight reduction in cost to \$1.17. With both the EMS-1 and the load-following strategies, fuel consumption is the same but the load-following strategy reduced the degradation of the battery and increased the FC degradation.

7. PFCV Cost Analysis

Short Urban drive cycles lead to reduced FC lifetimes and have high fixed costs from FC degradation. The cost per kilometre (\$/km), as shown in Table 7, reduces with increased drive cycle distance.

Table 7 Simulation results in \$ per km

		Urban	NEDC	WLTC	*VTS*TC
Distance	[km]	3.47	10.66	14.66	36.79
Cost (baseline-EMS)	[\$/km)]	0.113	0.076	0.069	0.074
Cost (EMS-1)	[\$/km)]	0.097	0.059	0.052	0.043

While the large 3.2 kWh battery in the FCV has sufficient capacity to complete short drive cycles in battery-only mode, there is no cost-advantage as the FC is the only battery recharging source. An alternative PFCV configuration is proposed which incorporates an on-board battery charger, similar to the 3-6 kW chargers found in battery electric vehicles. Research by [53] argues that a PFCV design would also reduce driver anxiety associated with a single fuel-source vehicle.

The offline analysis to calculate an equivalent cost to provide 1 kWh to the dc link from a battery which is charged from an external supply, must include the local electrical tariffs, charger efficiency and battery degradation costs during discharging and charging. Electricity tariffs are highly dependent on regional factors and range from \$0.10 to \$0.33 per kWh (USA average \$0.21 /kWh and UK average \$0.22 /kWh) [54]. An analysis of battery charging test data for the Nissan LEAF (2013 model) show the average charging efficiency is 89 % when recharging the battery at power levels from 3 kW to 6 kW [55]. The charging battery degradation costs calculated using (10,12,14,21) are shown in Fig. 9. Using the new battery degradation model, battery discharge gradation costs can be minimised by restricting the battery-only (charge-depletion) operation of the vehicle to SOC

values in the range of 50 % to 80 %. Assuming an on-board charger power rating of 4 kW and the specified battery-only SOC range, the average battery charging degradation cost is approximately \$0.0225/kWh.

This PFCV model configuration, with the initial SOC set to 80 %, costs \$0.075 /km for the Urban drive cycle, assuming the highest electrical utility tariff of \$0.33/kWh. This is a cost reduction of 22 % compared to the FCV operated using EMS-1 for the Urban drive cycle. At the end of the drive cycle, the battery DOD is only 20 %.

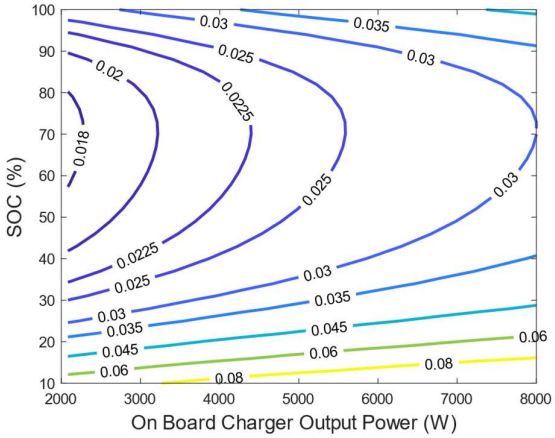

Fig. 9. *Battery charge degradation costs per kWh*

Over the longer NEDC drive cycle, the PFCV model cannot achieve battery-only operation within the 50-80% SOC range as the longer distance would result in a DOD of 55%. Operating initially on battery-only until the DOD is 30 % and then switching to a charge-sustaining strategy, a cost reduction (compared to EMS-1 costs) is only achieved if the electrical tariff is less than \$0.31/kWh. Further analysis and simulations of the PFCV model with the specified 3.2 kWh battery, show that COO costs are optimised if an on-board charger recharges the battery from an external supply for all journeys with distances up to 10 km. The PFCV strategy impacts the lifetime of both power sources. Battery lifetime in the PFCV is shorter than in the FCV due to the increase in battery power needed to complete journeys. The calculated battery lifetime for Urban drive cycles is 2182 h, while NEDC type drive cycles achieve battery lifetimes of 2665 h. The advantage of the PFCV model is seen in increased FC lifetime for Urban drive cycles, from 394 h (using EMS-1 in the FCV) to 1200 h in the PFCV.

8. Conclusions

This paper reports on the development of an EMS for a fuel cell-battery HEV to meet the requirements of the 2017 VTS challenge. The developed EMS, (EMS-1), for low traction power, operates the FC at a maximum efficiency power level to provide the average traction power and any surplus FC power is used to recharge the battery. For higher traction powers, EMS-1 implements a battery charge-sustaining strategy which allows the FC power output to increase linearly with traction power. The rule-based strategy is developed using offline optimisation in Matlab. EMS-1 achieves a drive cycle cost that is 2% lower than the winning challenge strategy while achieving prolonged lifetimes for both the FC and the battery.

The competition model is then modified to reflect the 2015 Toyota Mirai FCV, and a new battery degradation model is proposed for the vehicle which allows a charge-sustaining strategy at the battery SOC level commonly used in HEV and FCV designs.

Finally, the high cost for short drive cycles is addressed by proposing a PFCV design which reduces battery-only operation costs by recharging from a utility supply.

9. References

[1] C. Dépature, S. Jemeï, L. Boulon *et al.*, "IEEE VTS Motor Vehicles Challenge 2017 – Energy Management of a Fuel Cell / BatteryVehicle," in *IEEE Vehicle Power and Propulsion Conference*, Hangzhou, China, 2016.

[2] M. Ehsani, Y. Gao, S. Longo *et al.*, *Modern Electric, Hybrid Electric, and Fuel Cell Vehicles*. (CRC Press, 3rd edn. 2018).

[3] C. Mi, M. Abul Masrur, and D. Wenzhong Gao, *Hybrid Electric Vehicles Principles and Applications with Practical Perspectives*. (John Wiley & Sons, 1st edn. 2011).

[4] J. G. Hayes and G. A. Goodarzi, *Electric Powertrain:Energy Systems, Power Electronics and Drives for Hybrid,Electric and Fuel Cell Vehicles*. (John Wiley & Sons,1st edn. 2018).

[5] S. Ahmadi, S. M. T. Bathaee, and A. H. Hosseinpour, "Improving fuel economy and performance of a fuel-cell hybrid electric vehicle (fuel-cell, battery, and ultra-capacitor) using optimized energy management strategy," *Energy Convers. Manag.*, vol. 160, pp. 74–84, 2018.

[6] G. Wang, Y. Yu, H. Liu *et al.*, "Progress on design and development of polymer electrolyte membrane fuel cell systems for vehicle applications: A review," *Fuel Process. Technol.*, vol. 179, pp. 203–228, 2018.

[7] T. Yoshida and K. Kojima, "Toyota MIRAI Fuel Cell Vehicle and Progress Toward a Future Hydrogen Society," *Interface Mag.*, vol. 24, pp. 45–49, 2015.

[8] H. Lohse-Busch, M. Duoba, K. Stutenberg *et al.*, "Technology Assessment of a Fuel Cell Vehicle : 2017 Toyota Mirai," 2018.

[9] Y. Hames, K. Kaya, E. Baltacioglu et al., "Analysis of the control strategies for fuel saving in the hydrogen fuel cell vehicles," *Int. J. Hydrogen Energy*, vol. 43, pp. 10810–10821, 2018.

[10] I.-A. Alexa, S. Daniel Puscasu, and A. Onea, "Dynamic programming for energy management of hybrid energy supply system of electric vehicles," in *IEEE International Conference on Automation, Quality and Testing, Robotics*, Cluj-Napoca, Romania, 2018, pp. 1–6.

[11] K. Palmer, J. E. Tate, Z. Wadud *et al*., "Total cost of ownership and market share for hybrid and electric vehicles in the UK , US and Japan," *Appl. Energy*, vol. 209, pp. 108–119, 2018.
[12] J. Hagman, S. Ritzen, J. J. Stier *et al*., "Total cost of ownership and its potential implications for battery electric vehicle diffusion," *Res. Transp. Bus. Manag.*, vol. 18, pp. 11–17, 2016.
[13] E. a. Gilmore and L. B. Lave, "Comparing resale prices and total cost of ownership for gasoline, hybrid and diesel passenger cars and trucks," *Transp. Policy*, vol. 27, pp. 200–208, May 2013.
[14] S. Kara, W. Li, and N. Sadjiva, "Life Cycle Cost Analysis of Electrical Vehicles in Australia," *Procedia CIRP*, vol. 61, pp. 767–772, 2017.
[15] N. Sulaiman, M. A. Hannan, A. Mohamed *et al*., "Optimization of energy management system for fuel-cell hybrid electric vehicles: Issues and recommendations," *Appl. Energy*, vol. 228, no. July, pp. 2061–2079, 2018.
[16] J. J. Eckert, L. C. A. Silva, E. S. Costa *et al*., "Electric vehicle drivetrain optimisation," *IET Electr. Syst. Transp.*, vol. 7, no. 1, pp. 32–40, 2017.
[17] H. Li, A. Ravey, A. N. Diaye *et al*., "Equivalent consumption minimization strategy for hybrid electric vehicle powered by fuel cell , battery and supercapacitor," *IEEE Ind. Electron. Soc. Conf*, Florence, Italy, 2016, pp. 4401–4406.
[18] S. Onori, L. Serrao, and G. Rizzoni, *Hybrid Electric Vehicles Energy Management Strategies*. (SpringerBriefs in Control,Automation and Robotics,1st edn. 2016).
[19] S. H. Mahyiddin M. R. Mohamed, Z. Mustaffa *et al.*, "Fuzzy logic energy management system of series hybrid electric vehicle," in *IET Clean Energy and Technology Conference*, Kuala Lumper, Malaysia, 2016, pp. 1–6.
[20] W. Lee and H. Jeoung, "An Adaptive Energy Management Strategy For Extended-Range Electric Vehicles Based On Pontryagin ' s Minimum Principle," in *IEEE Vehicle Power and Propulsion Conference*, 2018, pp. 1–4.
[21] Z. Chen, N. Guo, Q. Zhang *et al*., Xiao, "An Optimized Rule Based Energy Management Strategy for a Fuel Cell / Battery Vehicle," in *IEEE Vehicle Power and Propulsion Conference*, Belfort, France, 2017.
[22] J. M. Lujan, C. Guardiola, B. Pla *et al*., "Analytical Optimal Solution to the Energy Management Problem in Series Hybrid Electric Vehicles," *IEEE Trans. Veh. Technol.*, vol. 67, no. 8, pp. 6803–6813, 2018.
[23] L. Serrao, S. Onori, A. Sciarretta *et al*., "Optimal energy management of hybrid electric vehicles including battery aging," in *American Control Conference*, San Franciso, USA, 2011, pp. 2125–2130.
[24] M. Carignano, V. Roda, R. Costa-Castelló *et al*., "Assessment of Energy Management in a Fuel Cell / Battery Hybrid Vehicle," *IEEE Access*, vol. 7, 2019.
[25] C. Dépature, S. Jemei, L. Boulon *et al.*, "Energy Management in Fuel-Cell/Battery Vehicles," *IEEE Vehicular Technology Magazine*, no. September, pp. 144–151, 2018.
[26] E. G. Amaya, C. De Angelo, and M. Asensio, "The Energy Management Strategy of FC / Battery Vehicles Winner of the 2017 IEEE VTS Motor Vehicles Challenge," in *IEEE Vehicle Power and Propulsion Conference*, Befort, France, 2017.
[27] A. Serpi, M. Porru, and A. F. Cell, "A Real-Time Energy Management System for Operating Cost Minimization of Fuel Cell / Battery Electric Vehicles," in *IEEE Vehicle Power and Propulsion Conference*, Belfort, France, 2017, pp. 2–6.
[28] M. Yue, S. Jemei, R. Gouriveau *et al*., "Developing a Health-Conscious Energy Management Strategy based on Prognostics for a Battery / Fuel cell Hybrid Electric Vehicle," in *IEEE Vehicle Power and Propulsion Conference*, Chicago, 2018, pp. 1–6.
[29] K. Kaya and Y. Hames, "Two new control strategies : For hydrogen fuel saving and extend the life cycle in the hydrogen fuel cell vehicles," *Int. J. Hydrogen Energy*, 2018.
[30] J. Chen, "Adaptive Fuzzy Logic Control of Fuel-Cell-Battery Hybrid Systems for Electric Vehicles," *IEEE Trans. Ind. Informatics*, vol. 14, no. 1, pp. 292–300, 2018.
[31] P. Pei and H. Chen, "Main factors affecting the lifetime of Proton Exchange Membrane fuel cells in vehicle applications: A review," *Appl. Energy*, vol. 125, pp. 60–75, 2014.
[32] P. Pei, Q. Chang, and T. Tang, "A quick evaluating method for automotive fuel cell lifetime," *Int. J. Hydrogen Energy*, vol. 33, pp. 3829–3836, 2008.
[33] Y. Yu, H. Li, H. Wang *et al*., "A review on performance degradation of proton exchange membrane fuel cells during startup and shutdown processes : Causes , consequences , and mitigation strategies," *J. Power Sources*, vol. 205, pp. 10–23, 2012.
[34] G. Wang, F. Huang, Y. Yu *et al*., "Degradation behavior of a proton exchange membrane fuel cell stack under dynamic cycles between idling and rated condition," *Int. J. Hydrogen Energy*, vol. 3, pp. 4471–4481, 2018.
[35] T. Zhang, P. Wang, H. Chen *et al*., "A review of automotive proton exchange membrane fuel cell degradation under start-stop operating condition," *Appl. Energy*, vol. 223, pp. 249–262, 2018.
[36] X. Jin, A. P. Vora, V. Hoshing *et al.*, "Comparison of Li-Ion Battery Degradation Models for System Design and Control Algorithm Development," in *American Control Conference*, Seattle, USA, 2017, pp. 74–79.
[37] J. Jaguemont, L. Boulon, P. Venet *et al*., "Lithium-Ion Battery Aging Experiments at Subzero Temperatures and Model Development for Capacity Fade Estimation," *IEEE Trans. Veh. Technol.*, vol. 65, no. 6, pp. 4328–4343, 2016.
[38] J. Wang J. Purewal, P. Liu *et al.*, "Degradation of lithium ion batteries employing graphite negatives and nickel - cobalt - manganese oxide + spinel manganese oxide positives : Part 1 , aging mechanisms and life estimation," *J. Power Sources*, vol. 269, pp. 937–948, 2014.
[39] M. Dubarry, N. Qin, and P. Brooker, "Calendar aging of commercial Li-ion cells of different chemistries – A review," *Curr. Opin. Electrochem.*, vol. 9, pp. 106–113, 2018.
[40] L. Serrao, S. Onori, and G. Rizzoni, "A Novel Model-Based Algorithm for Battery Prognosis," *IFAC Proc. Vol.*, vol. 42, no. 8, pp. 923–928, 2009.
[41] J. Wang, P. Liu, J. Hicks-garner *et al.*, "Cycle-life model for graphite-LiFePO 4 cells," *J. Power Sources*, vol. 196, no. 8, pp. 3942–3948, 2011.
[42] L. Serrao and Z. Chehab, "An Aging Model of Ni-MH Batteries for Hybrid Electric Vehicles," in *IEEE Vehicle Power and Propulsion Conference*, Chicago, USA, 2005, pp. 78–85.
[43] V. Marano, S. Onori, Y. Guezennec *et al*., "Lithium-ion batteries life estimation for plug-in hybrid electric vehicles," *IEEE Veh. Power Propuls. Conf.*, Dearborn, USA, 2009, pp. 536–543.
[44] E. Wikner, "Lithium ion Battery Aging : Battery Lifetime Testing and Physics-based Modeling for Electric Vehicle Applications," PhD. Thesis, CHALMERS UNIVERSITY OF TECHNOLOGY, Sweden, 2017.
[45] M. Chen and G. A. Rincon-Mora, "Accurate Electrical Battery Model Capable of Predicting Runtime and I – V Performance," *IEEE Trans. Energy Convers.*, vol. 21, pp. 504–511, 2006.
[46] "Tazzari Zero 2009 Specification." [Online]. Available: web.archive.org/web/20110626072432/http://tazzari-zero.com/ public/pdf/Zero 2009 ENG.pdf. [Accessed: 05-May-2019].
[47] K. Davis and J. G. Hayes, "Energy Management Strategy Development to Minimize the Operating Costs for a Fuel Cell Vehicle," in *IEEE Vehicle Power and Propulsion Conference*, Belfort, France, 2017.
[48] M. Matsunaga, T. Fukushima, and K. Ojima, "Powertrain System of Honda FCX Clarity Fuel Cell Vehicle," *World Electr. Veh. J.*, vol. 3, pp. 820–829, 2009.
[49] "Toyota Mirai Specification." [Online]. Available: https://toyotanews.pressroom.toyota.com/releases/2017+toyota+mirai+product.htm. [Accessed: 05-May-2019].
[50] B. K. Hong and S. H. Kim, "Recent Advances in Fuel Cell Electric Vehicle Technologies of Hyundai," *ECS Trans.*, vol. 86, no. 13, pp. 3–11, 2018.
[51] Y. Nonobe, "Development of the Fuel Cell Vehicle Mirai," *IEEJ Trans. Electr. Electron. Eng.*, vol. 12, pp. 5–9, 2017.
[52] T. Suzuki, "Fuel Cell Stack Technology of Toyota," *ECS Trans.*, vol. 75, no. 14, pp. 423–434, 2016.
[53] R. Alvarez Fernandez, F. Beltran Cilleruelo, and I. Villar Martinez, "A new approach to battery powered electric vehicles : A hydrogen fuel-cell-based range extender system," *Int. J. Hydrogen Energy*, vol. 41, pp. 0–11, 2016.

[54] Statista, “Electricity prices around the world 2018 | Statista,” 2019. [Online]. Available: www.statista.com/statistics/263492/ electricity-prices-in-selected-countries/.[Accessed: 05-May-2019].
[55] ANL, “Downloadable Dynamometer Database.” [Online]. Available: www.anl.gov/es/downloadable-dynamometer-database. [Accessed: 15-Jan-2019].